F. Campagnolo, V. Petrovic, J. Schreiber, E.M. Nanos, A. Croce, C.L. Bottasso
Wind Tunnel Testing of a Closed-Loop Wake Deflection Controller for Wind Farm Power Maximization
Journal of Physics: Conference Series, Vol. 753, 2016, 032006 (7 pages)
doi:10.1088/1742-6596/753/3/032006

Wind tunnel testing of a closed-loop wake deflection controller for wind farm power maximization

2016 J. Phys.: Conf. Ser. 753 032006

(http://iopscience.iop.org/1742-6596/753/3/032006)

Wind tunnel testing of a closed-loop wake deflection controller for wind farm power maximization

Filippo Campagnolo[1], Vlaho Petrović[1], Johannes Schreiber[1], Emmanouil M. Nanos[1], Alessandro Croce[2] and Carlo L. Bottasso[1,2]

[1] Wind Energy Institute, Technische Universität München, Boltzmannstraße 15, D-85748 Garching bei München, Germany

[2] Dipartimento di Scienze e Tecnologie Aerospaziali, Politecnico di Milano, Via La Masa 34, I-20156 Milano, Italy

E-mail: `filippo.campagnolo@tum.de`

Abstract. This paper presents results from wind tunnel tests aimed at evaluating a closed-loop wind farm controller for wind farm power maximization by wake deflection. Experiments are conducted in a large boundary layer wind tunnel, using three servo-actuated and sensorized wind turbine scaled models. First, we characterize the impact on steady-state power output of wake deflection, achieved by yawing the upstream wind turbines. Next, we illustrate the capability of the proposed wind farm controller to dynamically driving the upstream wind turbines to the optimal yaw misalignment setting.

1. Introduction

Wind energy production is often organized in wind power plants rather than single isolated wind turbines, because of lower construction, maintenance and commissioning costs. However, the design of a wind farm requires taking into account the complex interactions that take place within the wind power plant itself, since the wakes of upwind wind turbines have a strong impact on the power and loading of downstream machines. In recent years, interest has grown in the area of cooperative control of wind turbines, with the goal of maximizing the total wind farm power output, of achieving a given power setpoint while minimizing fatigue loading, or others that require some form of coordination among the wind turbines.

Among the several approaches investigated so far [7], controlling the direction of the wake by yawing the upwind wind turbines seems to be the most promising one [6]. In fact, by redirecting the wake, one may reduce or eliminate altogether the exposure of downwind wind turbines to the wakes shed upstream. In this paper, we present results obtained by testing a closed-loop wind farm control algorithm in a large boundary layer wind tunnel [3] using servo-actuated and sensorized wind turbine models, described in §2. The model-free controller, which optimizes online the yaw misalignment of the upstream wind turbines to increase the total wind farm power output, is discussed in §3, while results are reported in §4.

2. Experimental setup

Tests were conducted with a scaled wind farm (see Fig. 1) composed of three identical scaled wind turbine models with a rotor diameter of 1.1 m (in the following named G1s). The undisturbed

wind speed was measured by means of a Pitot tube, also shown in the figure, placed at hub height and 3 diameters in front of the upstream model.

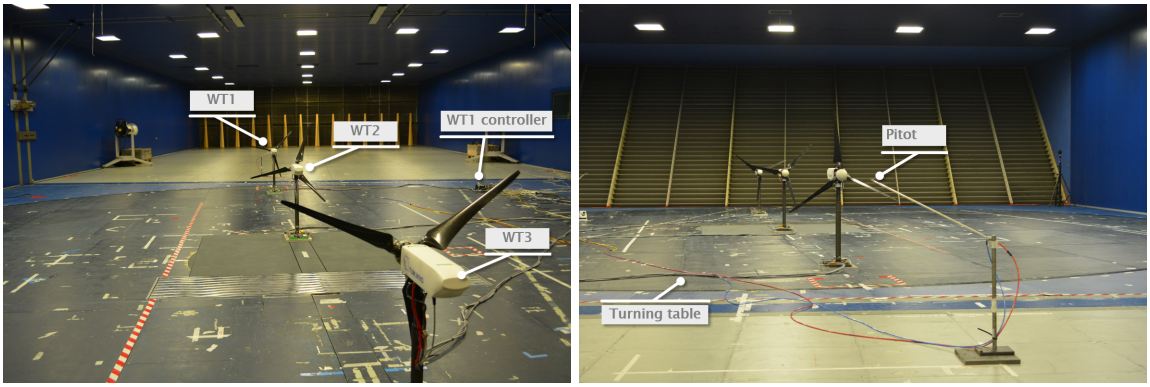

Figure 1: Wind farm layout in the wind tunnel

Each `G1` (see Fig. 2), whose rated rotor speed is 850 rpm, is equipped with three blades, which are composed by a layer of unidirectional carbon fiber covering a machined Rohacell core, mounted on the hub with two bearings in order to enable pitch actuation while limiting free-play. The individual pitch angle of each blade can be varied by means of a small brushed motor equipped with a gearhead and built-in relative encoder, used to measure the blade pitch. The three motors are housed within the blades hollow root, and their position is monitored and adjusted by dedicated electronic control boards housed in the hub spinner.

The shaft is held by two bearings, in turn housed in the rectangular carrying box that constitutes the main frame of the nacelle. The shaft also exhibits four small bridges on which strain gages are glued, to provide measurements of the torsional and bending loads. Three miniaturized electronic boards, fixed to the hub, provide for the power supply and conditioning of the shaft strain gages. The transmission of the electrical signals from the rotating system to the fixed one, and vice versa, is guaranteed by a through-bore 12-channels slip ring.

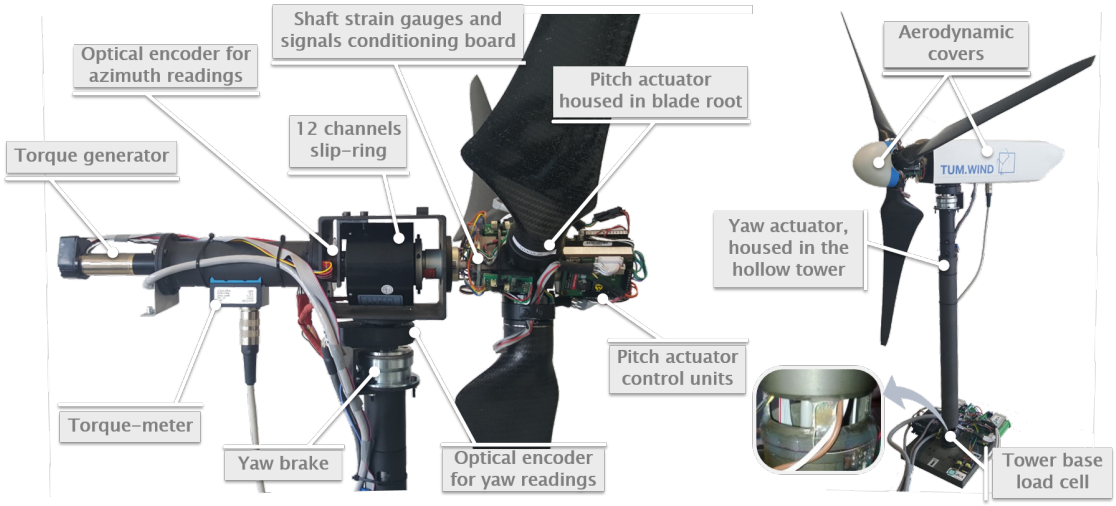

Figure 2: Layout of G1 model

A torque-meter, located after the two shaft bearings, allows for the measurement of the torque provided by a brushless motor equipped with a gearhead and a tachometer. The motor, located

in the rear part of the nacelle, is operated as a generator by using a servocontroller. An optical encoder, located between the slip ring and the rear shaft bearing, allows for the measurement of the rotor azimuth.

The entire nacelle can be yawed by means of a brushed motor, housed within the hollow tower, equipped with a gearhead. This latter element is connected by a multi-beam coupling to a shaft rigidly joined to the rectangular carrying box, and hold in place by two bearings located within the upper portion of the tower. An optical encoder provides feedback to an electronic device that controls both the yaw actuator and a magnetic brake.

The tower, whose stiffness was designed so that the first fore-aft and side-side natural frequencies of the nacelle-tower group are properly placed with respect to the harmonic per-rev excitations, is softened at its base by machining four small bridges, on which strain gages are glued. Bridges were sized so as to have sufficiently large strains to achieve the necessary level of accuracy for the strain gages. Two electronic boards provide for the power supply and adequate conditioning of this custom-made load cell.

Aerodynamic covers of the nacelle and hub ensure a satisfactory quality of the flow in the central rotor area

Due to the small dimensions of the scaled wind turbine, low Reynolds numbers are expected. Therefore, the low-Reynolds airfoil RG14 [8] was chosen for the model wind turbine blades. The aerodynamic performance of the rotor was measured for different values of the airfoil Reynolds by operating the models at several combinations of tip speed ratio (TSR) and collective pitch settings. The measured maximum power coefficients are approximately 0.42 at $\lambda \in [7, 8]$ and $\beta \in [-2°, 0°]$.

3. Control system

The control system of the wind turbine models is organized in three different levels, as shown in Fig. 3. The low level control operates the wind turbine actuators, while the communication with sensors, actuators, and control algorithms are implemented on the industrial real-time controller Bachmann M1 (http://www.bachmann.info). Wind farm control algorithms, as well as supervisory control for each model, are implemented on a standard PC, which communicates with each wind turbine controller over an Ethernet network.

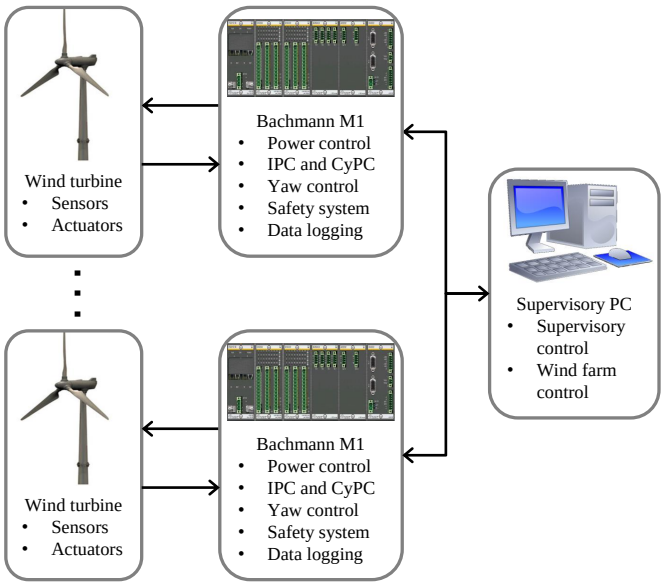

Figure 3: Control structure of the wind turbine models.

3.1. Wind turbine control system

The Bachmann M1 system used for wind turbine control is a modular real-time controller with a CPU module for running control algorithms, a counter module for acquiring rotor speed and azimuth from the digital encoder, a communication module for communication with actuators through a CAN network and two analogue input-output modules for acquiring measurements and sending commands to the torque motor and the yaw break. The Bachmann M1 system is capable of acquiring data with a sample rate of 2.5 kHz, which is used for acquiring aerodynamic torque, shaft bending moments and rotor azimuth position. All other measurements are acquired with a sample rate of 250 Hz.

Each wind turbine model is controlled by a separate Bachmann M1 system with a sampling time of 4 ms. Besides data-logging and safety systems (such as shutdown in case of overspeed), the following control algorithms are implemented on each M1 system:

- **Power control, i.e. torque and collective pitch control (CPC).** A standard power control is implemented based on [1], with two distinct control regions. In the region below rated wind speed, blade pitch angles are kept constant, while the generator torque reference follows a quadratic function of rotor speed in order to maximize energy extraction. Above rated wind speed, the generator torque is kept constant, while a PI controller is used to collectively pitch the rotor blades in order to keep the generated power at the desired level. Additionally, for the purpose of wind farm control, the wind turbine power output can be lowered to an arbitrary percentage of the available power below rated wind speed and of the nominal power above rated wind speed. Since power reduction can be achieved in different ways, it is possible to easily modify the control trajectories while the models are idling.
- **Individual and cyclic pitch control (IPC and CyPC).** Besides collective pitch control, the models are also capable of individually pitching each blade, enabling additional control actions for influencing loading or wakes. To this aim, the reference of each blade follows a harmonic function of the blade azimuth position with adjustable amplitude and phase angle. This leads to continuous blade pitching with frequency 1P, whose maximal amplitude has to be constrained according to the pitch actuator capabilities. This kind of pitch activity has a strong impact on loads, while the generated power remains unaffected above rated wind speed. On the other hand a slight power loss can be observed below rated wind speed, depending on the pitch amplitude [2, 11]. The amplitude and the phase angle of the blade pitch can be determined either in close loop by two decoupled PI controllers trying to reduce 1P oscillations of the shaft bending moments (IPC, for more details see [10]), or in open loop (CyPC).
- **Yaw control.** The misalignment angle of a wind turbine model with respect to the wind can be set by changing the yaw angle. A PI controller is used for controlling the yaw motor, and the yaw reference value is provided from the supervisory controller. An additional control logic is implemented that enables the yaw brake once the nacelle gets in the desired position. Whenever the yaw reference is changed, the brake is released and the PI controller ensures that the nacelle is yawed to the new position. Besides constant yaw references, the yaw controller is also capable of continuous yaw motion, such as a harmonic function with adjustable amplitude and frequency. Such a motion can be useful for wind farm control algorithms or for the generation of wake meandering in the wind tunnel.

3.2. Wind farm control system

High level control is implemented on a standard PC, and communication with the wind turbine Bachmann M1 controllers is established over an Ethernet network. Through a dedicated graphic interface, the supervisory controller allows for the user to monitor the wind turbine conditions, change their operating state, control algorithms and reference values, and to set up and initialize

the data acquisition process. Additionally, a wind farm control algorithm collects measurements from the Bachmann M1 controllers, and can send the following control actions back to them:

- a command to reduce produced power,
- a yaw angle reference,
- CyPC settings.

The wind turbine controller described in §3.1 is in charge of following the references sent by the wind farm controller.

At present, a gradient-based extremum seeking control algorithm is implemented with the goal of increasing energy capture. Gradients are computed by first-order finite differencing the energy capture, properly averaged over a time horizon, at two different wind turbine operating points. The control algorithm is based on [5], where yaw misalignment optimization is performed rather than axial induction. The algorithm uses the simplified assumption that control actions of a wind turbine affect only the closest downstream wind turbine. Therefore, instead of solving a single optimization problem for the entire wind farm, a series of smaller optimization problems (one for each wind turbine) is being solved:

$$\gamma_i^* = \arg\max_{\gamma} P_i + P_{i+1}. \tag{1}$$

The optimal yaw angle γ_i^* is therefore determined based on the power output of the i^{th} wind turbine P_i and its closest downwind neighbor, P_{i+1}. The optimization problems are suitably synchronized by waiting for the propagation of the wakes only to the neighboring wind turbines, thus significantly reducing the convergence time of the algorithm. The time required for the wake to propagate is computed online using Jensen's model to estimate the speed in the wake. The average wind speed measured by the Pitot tube described earlier is used as input to the Jensen's model. The axial induction factor is computed by properly non-dimensionalizing the rotor thrust, in turn derived from the fore-aft bending moment measured at tower base, using the well-known relationship

$$C_T = 4a(1-a). \tag{2}$$

The wake decay coefficient is obtained by best-fitting experimental data from previous wind tunnel tests [4].

Although such an approach changes the original objective (power maximization in the entire wind farm), and therefore could result in suboptimal performance, it can also lead to significantly faster convergence.

4. Results

Tests were conducted by simulating the atmospheric boundary layer by means of spires placed at the inlet of the wind tunnel, in order to generate a wind speed vertical profile and turbulence intensity typical of offshore applications.

The machines were arranged with a flow-wise longitudinal spacing of 4 diameters and a laterally shift of half a diameter, as depicted in Fig. 1. The average wind speed measured by the Pitot tube described earlier is used to derive the wind turbine and wind farm power coefficients, the latter being defined as the sum of the wind turbine ones.

At first, different combinations of yaw misalignment for the upstream ($WT1$) and second ($WT2$) wind turbine model were tested within the wind tunnel, with the aim of experimentally identifying the operating condition maximizing wind farm power output. Figure 4 shows that, for the tested wind farm layout and wind condition, wind farm power can be substantially increased (up to 15%) by misaligning $WT1$ and $WT2$ of approximately 20 deg and 16 deg, respectively.

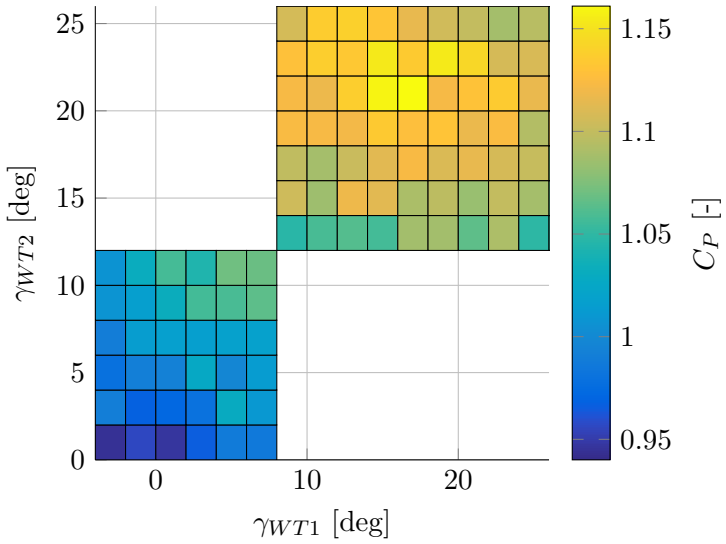

Figure 4: Measured wind farm power coefficient C_P as function of upstream WT yaw misalignment (γ_{WT1}) WT yaw misalignment (γ_{WT1}).

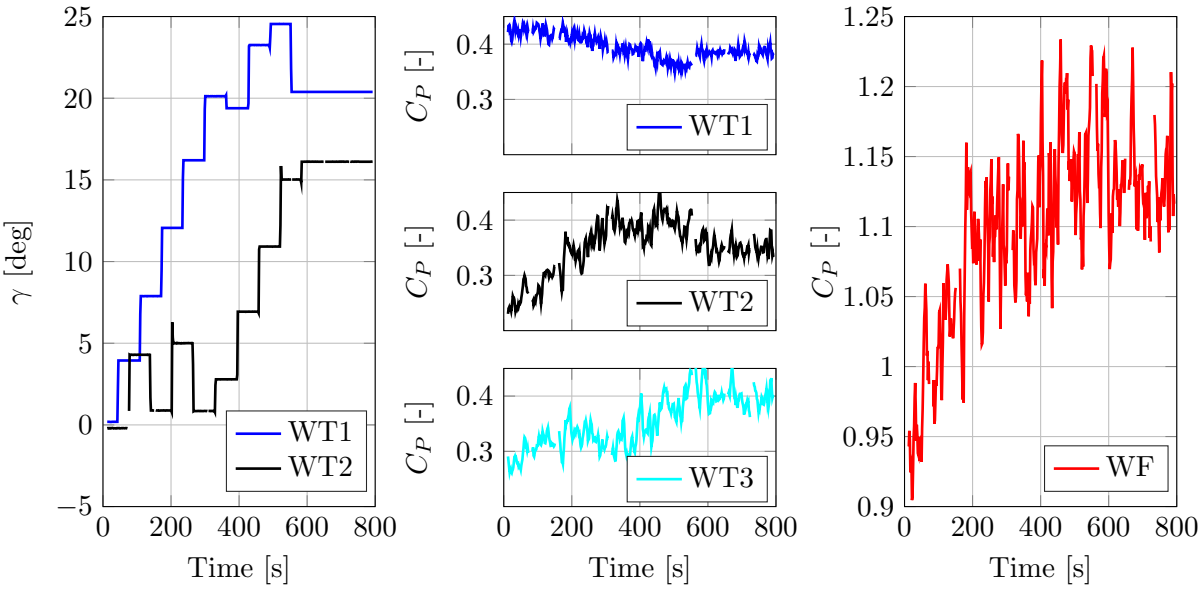

Figure 5: WTs yaw misalignment (on left), WTs power coefficient (center) and wind farm power coefficient as function of time (right)

.

Figure 5 shows the time evolution of the upstream WT yaw misalignments, as well as the evolution of the power coeffient for the three wind turbines and the whole wind farm, after the activation of the proposed wind farm controller. The data reported in Fig. 5 clearly highlights that the wind farm controller is capable of dynamically driving the wind turbines to yaw misalignment settings that, based on the results shown in Fig. 4, maximize the wind farm power output. This leads to an increase of power in excess of 15%, a result which is in line with what reported by other authors using simulations [6] and wind tunnel testing [9].

5. Conclusions

A closed-loop model-free controller has been developed and tested in a large boundary layer wind tunnel, where one can simulate wind conditions typical of offshore applications. Thanks to the use of sophisticated wind turbine models, extensively instrumented and equipped with individual pitch, torque and yaw control, it has been experimentally demonstrated that wake redirection by means of yaw misalignment can lead to substantial increase in wind farm power output. Moreover, it was shown for the first time that a closed-loop wind farm controller is capable of dynamically driving the upstream wind turbines to the optimal operational conditions.

Acknowledgments

This work was financially supported by the German Federal Ministry for Economic Affairs and Energy (BMWi) within the CompactWind project (FKZ 0325492D).

References

[1] Bossanyi E 2000 *Wind Energy* **3** 149–163
[2] Bossanyi E 2005 *Wind Energy* **8** 481–485
[3] Bottasso C L, Campagnolo, F and Petrović V 2014 *Journal of Wind Engineering and Industrial Aerodynamics* **127** 11–28
[4] Campagnolo F, Petrović V, Bottasso C L and Croce A 2016 *American Control Conference (ACC)* 513–518
[5] Gebraad P M Om van Wingerden J W, 2015 *Wind Energy* **18** 429–447
[6] Gebraad P M O, Teeuwisse FM, van Wingerden JW, Fleming PA, Ruben SD, Marden JR and Pao LY 2014 *Wind Energy* **19** 95–114
[7] Knudsen T, Bak T and Svenstrup M 2015 *Wind Energy* **18** 1333-1351
[8] Lyon C A, Broeren A P, Gigure P, Gopalarathnam A, Selig M S 1998 *SoarTech Publications* **3**
[9] Park J, Law K 2016 *IEEE Transactions on Control Systems Technology* **24** 1655-1668.
[10] Petrović V and Campagnolo F 2013 *European Control Conference 2013*, Zurich
[11] Petrović V, Jelavić M and Baotić M 2015 *Renewable Energy* **76** 418–431